12th International Conference on Fracture Mechanics of Concrete and Concrete Structures
FraMCoS-12
B.L.A. Pichler, Ch. Hellmich, P. Preinstorfer (Eds)

https://doi.org/10.21012/FC12.1132
MS01-2:3

SCALE EFFECTS INVESTIGATION ON THE MECHANICAL BEHAVIOUR OF STEEL-FIBRE AND STEEL-BAR (HYBRID) REINFORCED CONCRETE BEAMS

BINEET KUMAR, CHUANLIN WANG, YUZHONG LIU, SHUPENG ZHOU, QINGYOU OU, JUNKAI LIU, YING YU, FEDERICO ACCORNERO, ALBERTO CARPINTERI

Department of Civil Engineering and Smart Cities, Shantou University, Shantou 515063, Guangdong, China
e-mail: bineetkumar@stu.edu.cn

Key words: Updated Bridged Crack Model; Minimum reinforcement; Fibre volume fraction; Mechanical performance; Size-scale effects; Steel-fibre reinforced concrete

Abstract: This study investigates the mechanical behaviour of steel-fibre and steel-bar (hybrid) reinforced concrete (HRC) beams including flexural cracking, shear, and flexural crushing failure modes in the framework of Fracture Mechanics by means of the Updated Bridged Crack Model (UBCM). The experiments are carried out via four-point bending tests on 300 beams (3 identical specimens per 100 different cases) with: (1) longitudinal steel-bar percentages of 0.00, 0.06, 0.13, 0.28, and 0.50%; (2) fibre volume fractions of 0.00, 0.10, 0.20, 0.40, and 0.80%; (3) beam depths of 20, 40, 80, and 160 cm; (4) slenderness ratio constant and equal to 6. The UBCM is applied to assess crack propagation and failure mechanisms in hybrid-reinforced concrete beams. The reinforcement brittleness numbers (N_P and $N_{P,f}$) and the pull-out brittleness number (N_w) are thoroughly studied, and the numerical results prove that a softening post-cracking response of the hybrid-reinforced concrete element emerges, and its mechanical performance results to be scale-dependent. The numerical analyses prove the strong interaction between the two design parameters: steel-bar percentage and fibre volume fraction.

1 INTRODUCTION

Concrete is the most widely used and extensively applied construction material globally, characterized by its complexity, multi-layered structure, multiphase nature, and multiple constituent components. However, its inherent brittleness and low tensile strength significantly impact its practicality and limitations in real-world applications. The brittleness of concrete severely restricts its ductility, which is a critical measure of a material ability to absorb energy and undergo plastic deformation without failure [1,2]. In this research, scholars continuously explore novel fibre-reinforced concretes to enhance crack resistance and concrete strength. The incorporation of fibres can transform the failure mode of concrete from sudden brittle failure to ductile failure with precursors. Steel fibre-reinforced concrete, as a multiphase composite material, not only retains the excellent properties of ordinary concrete but also significantly improves its tensile strength, crack resistance, and toughness. When subjected to loads, micro-cracks develop within the concrete matrix. Steel fibres, possessing high elastic modulus and excellent interfacial bonding capabilities, can effectively transfer loads, thereby enhancing the overall performance of the concrete [3]. When the crack tip propagation path encounters steel fibres, it is compelled to alter its extension trajectory or evolve into finer cracks. As the cracks propagate, the extraction of steel fibres consumes a substantial amount of energy, thereby enhancing the material's toughness. The failure mode of HRC beams, as depicted in Figure 1, demonstrates that the incorporation of fibres in HRC beams reduces the quantity and width of shear cracks. Fibres contribute to the improvement of concrete ductility and delay fracture development.

To date, numerous models have been

proposed. The earliest model was introduced by Malvar, who developed the renowned Karagozian & Case (K&C) concrete model based on the finite element code DYNA3D [4]. Thai et al. calibrated this model, and the calibrated model can be used to describe the complex static and dynamic behaviours of fibre-reinforced concrete (FRC) structures under both static and high-speed loading conditions [5]. Additionally, the earliest fracture mechanics models were introduced to predict the tension softening experienced by materials such as concrete prior to crack propagation [6-8].

This paper employs the UBCM (Updated Bridged Crack Model) put forward by Carpinteri [9] to predict the flexural behaviour of HRC (Hybrid Reinforced Concrete) beams. A finite element algorithm is used to predict the size effect in the structural response of FRC (Fiber-Reinforced Concrete). This model allows for capturing the influence of each individual component of the composite material in the post-cracking state, assuming that the composite material is a multiphase material. Dimensionless numbers are used to describe the impact of different phases on the flexural response.

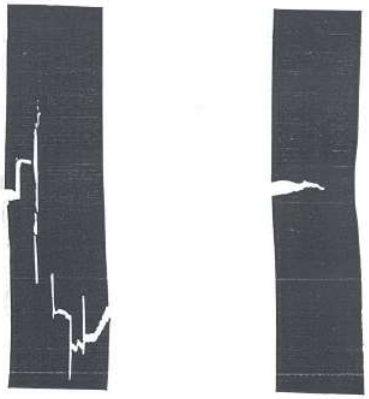

Figure 1: Crack development in fiber reinforced concrete (left) and in plain concrete (right).

2 UBCM

UBCM treats steel fiber-reinforced concrete (SFRC) components as homogeneous, linear-elastic, and fully brittle materials. The matrix adheres to Hooke's Law under external loading, exhibiting no significant plastic deformation and undergoing sudden fracture upon reaching the failure strength. Nonlinear contributions, such as those from fibres, are neglected during both tensile and compressive loading. The UBCM assumes that tensile cracking precedes other failure mechanisms, such as compressive crushing and shear failure, with a focus on the crack propagation phenomena at critical sections. The composite material, formed by the combination of steel fibres and concrete, is assumed by the UBCM to be a multiphase material, wherein the cementitious matrix and the reinforcement layer represent the primary and secondary phases, respectively, both contributing to the overall toughness of the structural element.

In the simulated four-point bending test, the loading methodology is depicted in Figure 2. Reinforcing layers act to bridge the cracks during the progression of crack propagation, with the toughening efficacy quantified by the distribution of the bridging force, described by Equation 1. The global stress intensity factor is determined in accordance with Equation 2 [10,11]. Crack extension commences when the stress intensity factor K_{I} attains the matrix fracture toughness K_{IC}. The local rotation of the beam due to crack opening and the overall deflection can be calculated using Equation 3, which incorporates the nonlinear cracking at the critical interface as well as the nonlinear cracking in the remaining elastic regions.

$$F_i = F(w_i) \tag{1}$$

$$K_I = K_i - \sum_{i=1}^{m} K_{Ii} \tag{2}$$

$$\begin{Bmatrix} \Delta\varphi \\ \delta \end{Bmatrix} = \begin{pmatrix} \lambda_{MM} & \lambda_{MF} \\ \lambda_{FM} & \lambda_{FF} \end{pmatrix} \begin{Bmatrix} M \\ F \end{Bmatrix} \tag{3}$$

Equation 1 affords a suite of m equations that establish the relationship between the stress exerted on the i-th active reinforcement layer. Within Equation 2, K_{i} signifies the contribution from the applied bending moment, whereas K_{Ii} indicates the contribution of the i-th reinforcing phase. In Equation 3, $\Delta\varphi$ and δrepresents the crack opening vector, λ_{M} denotes the local flexibility vector resulting from the bending moment, and λ_{F} signifies the local flexibility matrix arising from the bridging force.

The influences of the dimensionless numbers N_{P}, $N_{\mathrm{P,f}}$, N_{w} are considered, where

$N_{\mathrm{P}}$is the bar-reinforcement brittleness number, dependent on the reinforcement ratio; $N_{\mathrm{P,f}}$ is the fibre-reinforcement brittleness number, dependent on the fibre volume fraction; N_{w} is the pull-out brittleness number, dependent on the fiber volume fraction; [10,11]:

$$N_{\mathrm{P}} = \rho \frac{\sigma_y}{K_{\mathrm{IC}}} h^{1/2} \quad (4)$$

$$N_{\mathrm{P,f}} = V_f \frac{\widetilde{\sigma_s}}{K_{\mathrm{IC}}} h^{1/2} \quad (5)$$

$$N_{\mathrm{w}} = \frac{E w_c}{K_{\mathrm{IC}} h^{1/2}} \quad (6)$$

where V_f represents the fiber volume fraction, $\widetilde{\sigma_s}$ denotes the generalized bond strength of the fibers, h is the height of the beam, E is the Young's modulus, w_{c} is the equivalent embedment length of the fibers, ρ signifies the reinforcement ratio, and σ_{y} is the yield stress of the steel reinforcement.

3 TESTING SETUP

A four-point bending test was simulated, with the loading configuration as illustrated in Figure 2. The bending response was characterized by the dimensionless fracture moment and the locally normalized rotation [12]:

$$\widetilde{M_F} = \frac{M_F}{K_{IC} b h^{3/2}} \quad (7)$$

$$\tilde{\varphi} = \varphi \frac{E h^{1/2}}{K_{IC}} \quad (8)$$

In Equation 7, M_F represents the fracture moment, K_{IC} denotes the fracture toughness of the concrete, b is the thickness of the specimen, and h is the height of the component. In Equation 8, φ signifies the local rotation of the cross-section, and E is the Young's modulus.

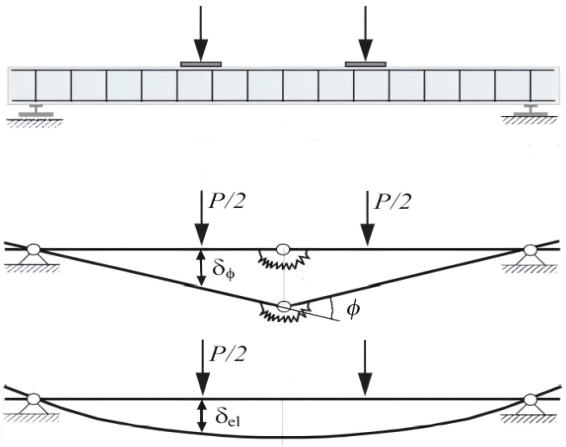

Figure 2: Elastic hinge due to the fracturing process.

The dimensions used in the simulation are as shown in Table1. The slenderness ratio of the components is 6, employing notched beams with a precast crack depth of h/10. The reinforcement ratios of the steel bars are 0.0%, 0.06%, 0.28%, and 0.50%. The fiber type utilized is hooked-end steel fiber, with fiber volume fractions of 0.0%, 0.1%, 0.2%, 0.4%, and 0.8%.The technical drawings of the beam and the loading configuration are illustrated in Figure 3.

Table 1: HRC beam geometry

	span	depth	width	Notch depth	Concrete strength
HRC200	1200	200	200	20	C30
HRC400	2400	400	200	40	C30
HRC800	4800	800	200	80	C30
HRC1600	9600	1600	400	160	C30

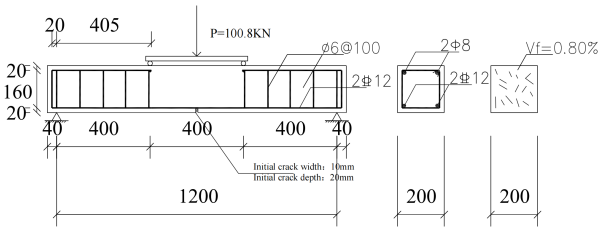

Figure 3: Reinforcement scheme.

4 NUMERICAL RESULTS

In Figures 4(a)-(e), the load-deflection diagrams are represented for N_{w} = 580, a different N_{P} value for each diagram, and parametrically varying $N_{\mathrm{P,f}}$ values. In Figure 4(a), N_{P} is equal to 0.00 (no steel-bars) and only

the first curve $N_{P,f}$ = 0.67 presents the same level for the two peak loads (first fracturing and ultimate load), i.e, the minimum reinforcement condition. Then, in the remaining diagrams, the peak load related to first cracking is higher than the ultimate load, leading to a brittle behaviour.

In Figure 4(b), N_P is equal to 0.15 and the two curves $N_{P,f}$ = 0.67 and 0.34 represent a ductile behaviour, whereas from $N_{P,f}$ = 0.17 to 0.00 they represent hyperstrength cases.

In Figure 4(c), N_P is equal to 0.27 and the three curves $N_{P,f}$ = 0.67, 0.34, and 0.17 represent a ductile behaviour, whereas $N_{P,f}$ = 0.08 and 0.00 represent hyperstrength cases.

In Figure 4(d), N_P is equal to 0.60 and all the curves represent a ductile behaviour (ultimate load always higher than first fracturing load).

In Figure 4(e), N_P is equal to 1.07 and all the curves represent a ductile behaviour. In addition, it is worth noting that the asymptotic value is closer to the ultimate load than in the previous cases, further increasing the ductility of the system.

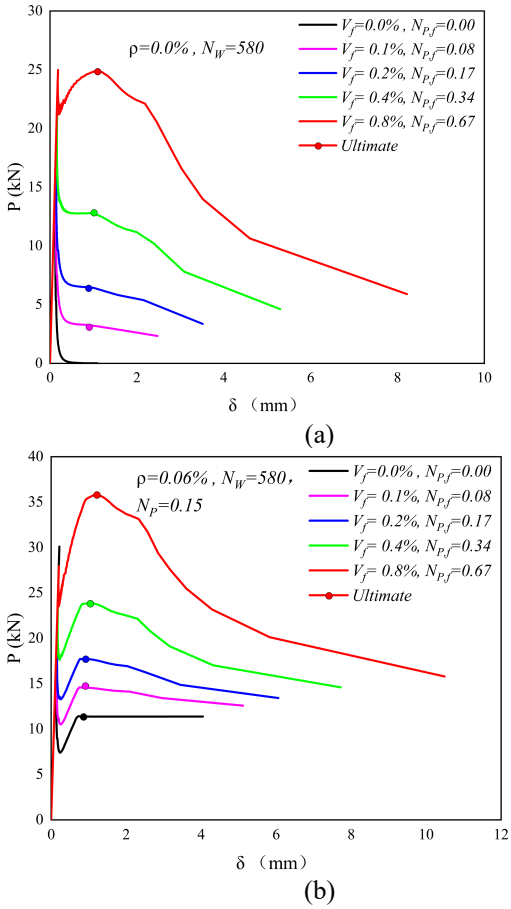

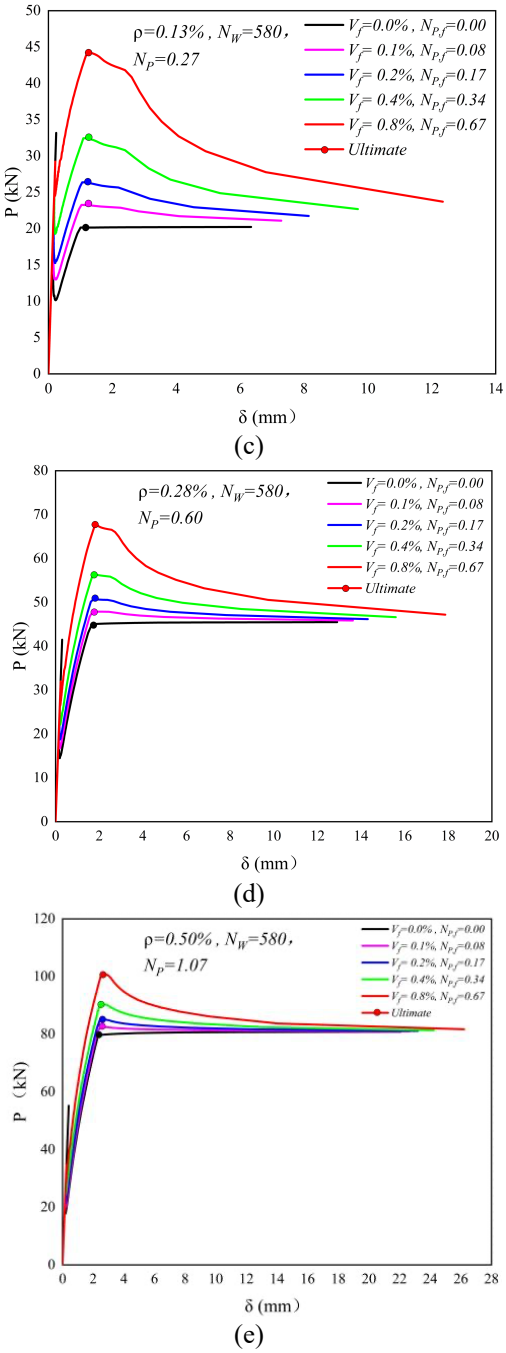

Figure 4: HRC200 load vs deflection.

In order to evaluate the minimum reinforcement conditions for HRC beams, each point of the diagram in Figure 5 corresponds to a combination of the two reinforcement brittleness numbers, N_P and $N_{P,f}$, required to obtain a stable post-peak response.

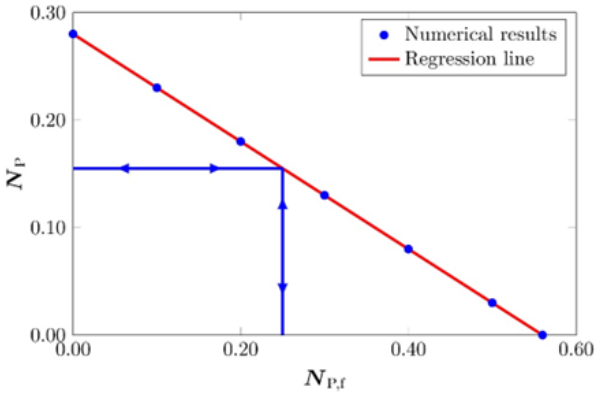

Figure 5: Minimum reinforcement conditions.

REFERENCES

[1] S. Dong, D. Zhou, A. Ashour, B. Han, J. Ou. Flexural toughness and calculation model of super-fine stainless wire reinforced reactive powder concrete. Cem. Concr. Compos., 104 (2019), Article 103367.

[2] X. Zhou, W. Zheng, Y. Zeng, C. Xu, P. Chen. Effect of fiber content and stress–strength ratio on the creep of basalt fiber–reinforced alkali-activated slag concrete. Struct. Concr., 23 (1) (2022), pp. 382-394

[3] YOO D Y,KIM J J,PARK JJ. Effect of fiber spacing on dynamic pullout behavior of multiple straight steel fibers in ultra-high-per- formance concrete[J]. Construction and Building Materials,2019,461-472

[4] L.Javier Malvar, John E. Crawford, James W. Wesevich, Don Simons,A plasticity concrete material model for DYNA3D,International Journal of Impact Engineering,Volume 19, Issues 9–10,1997,847-873.

[5] Duc-Kien Thai, Duy-Liem Nguyen, Duy-Duan Nguyen,A calibration of the material model for FRC,Construction and Building Materials,Volume 254,2020,119293

[6] Z.P. Bazant, P.A. Pfeiffer. Determination of fracture energy from size effect and brittleness number. ACI Mater. J., 84 (6) (1987), pp. 463-480

[7] Y.S. Jenq, S.P. Shah. A fracture toughness criterion for concrete. Engng. Fract. Mech., 21 (5) (1985), pp. 1055-1069

[8] A. Hillerborg, M. Modeer, P.-E. Petersson. Analysis of crack formation and crack growth in concrete by means of fracture mechanics and finite elements. Cem. Concr. Res., 6 (1976)

[9] A. Carpinteri, F. Accornero, A. Rubino, " Scale effects in the post-cracking behaviour of fibre-reinforced concrete beams", International Journal of Fracture, 2023, 240(1):1-16.

[10] F. Accornero, A. Rubino, A. Carpinteri, " Ultra-low cycle fatigue (ULCF) in fibre-reinforced concrete beams ", Theoretical and Applied Fracture Mechanics, 2022, 120:103392.

[11] F. Accornero, A. Rubino, A. Carpinteri, " Post-cracking regimes in the flexural behaviour of fibre-reinforced concrete beams", International Journal of Solids and Structures, 2022, 248:111637.

[12] F. Accornero, A. Rubino, A. Carpinteri, " A fracture mechanics approach to the design of hybrid-reinforced concrete beams", Engineering Fracture Mechanics, 2022, 275:108821.